CRACK RESISTANCE BEHAVIOUR OF A CrMoV PRESSURE VESSEL STEEL

E. SCHICK*, H. BLUMENAUER* and P. VEIT**
*Department of Materials Engineering and Materials Testing, Otto-von-Guericke University, D-39016 Magdeburg, Germany
**Department of Experimental Physics, Otto-von-Guericke University, D-39016 Magdeburg, Germany

ABSTRACT

The paper describes the influence of the microstructure of a CrMoV pressure vessel steel on the crack resistance curve J-Δa. Different heat treatment was used to change the microstructure essentially by variation of the carbide size, shape and distribution. Due to the change of the microstructure a different deformation behaviour is evident in the true stress-strain curves described by the Ramberg-Osgood law.

The crack resistance has been characterized by R-curves J-Δa using precracked SENB specimens. The varied microstructure influenced both the profile of the stretched zone and the elastic-plastic fracture parameters J_i and tearing modulus. The reason were found in a different damage development particularly by the interaction of the inclusions and the small second phase particles (carbides).

KEYWORDS

CrMoV pressure vessel steel, bainitic microstructure, R-curve J - Δa, stretched zone, crack initiation, crack growth

INTRODUCTION

Pressure vessels fabricated from low alloyed CrMoV steels are characterized by a very variable microstructure through the wall, depending on the cooling conditions after austenitization and the tempering parameters. Several investigations have shown, that this microstructural gradient is the reason for a wide range of the strength and toughness values (Ridley *et al.*,1994; Holzmann *et al.*,1995; Pointner, 1991; Thomson and Badeshia, 1994; Parilák and Dojcak, 1993). In order to estimate the reliability of the vessel by elastic-plastic fracture mechanics approaches a better understanding is necessary to explain the influence of the microstructure on the ductile fracture mechanism.

The ductile fracture in CrMoV steels is not only caused by formation of primary voids at the sulfides, but also by nucleation of secondary voids in the strain hardening matrix at the essentially smaller carbides (Tveergard, 1989; Li *et al.*, 1989; Deimel and Sattler, 1993; Tomita, 1995; Sun *et al.*, 1995). Therefore in this paper the influence of the carbides as second phase particles on the blunting and crack extension process is presented and discussed.

MATERIAL AND EXPERIMENTS

The material used in this investigation was the pressure vessel steel 17CrMoV10 in forged condition with the chemical composition C=0.17%, Cr=2.71%, Mo=0.14%, V=0.12%. Different heat treatment was used to change the precipitation state of the carbides, whereby the sulfides remain unchanged (content of sulphur 0.014%, medium diameter of sulfides d_{MnS}=3.56 µm, volume fraction f_v=0.0886 %). The heat treatment parameters and the mechanical properties of three microstructures B1,V1,V2 are presented in Table 1, and also the Ramberg-Osgood law with the coefficients α, N and the work hardening exponent n of the true stress-strain curve. An evident decrease of the n-values is connected with the increasing yield strength and decreasing notch impact energy.

TABLE 1 Heat treatment and mechanical properties

microstructure designation	heat treatment	R_e [MPa]	R_m [MPa]	Ramberg-Osgood-law	n	KV [J]
B1	isothermal bainitized: 950°C, 30 min, 5s/460°C, 2h, air 680°C, 2h, air	660	760	$\varepsilon/\varepsilon_o = 2.1(\sigma/\sigma_o)^{12.3}$	0.081	60
V1	quenched and tempered: 950°C/1h/oil/ 650°C/7 h/air	518	647	$\varepsilon/\varepsilon_o = 3.9(\sigma/\sigma_o)^{7.1}$	0.141	120
V2	as V1 + 680°C/ 160 h/air	385	548	$\varepsilon/\varepsilon_o = 3.9(\sigma/\sigma_o)^{5.6}$	0.178	170

For each heat treatment the microstructure is bainitic, consisting of a ferritic matrix with small carbides (Fig. 1). The precipitation state was investigated on extraction replicas and thin foils by TEM coupled with an image analysing system. The chemical composition of the carbides, their medium size, distribution and shape factor were estimated. The microstructure B1 obtained by isothermal transformation is characterized by very small particles, predominantly platelike vanadium carbides, mostly accumulated in the ferritic grains. Only the $M_{23}C_6$ particles are visible, especially on the boundaries of the bainitic laths. The carbide analysis for the microstructure V1 and V2 resulted in the same $M_{23}C_6$ type, mainly globular or prismatic, but also in the shape of thin rods and narrow ribbons. The medium size of the V2 carbides was larger, but the number of particles showed a decreasing trend. Molybdenum carbides were only

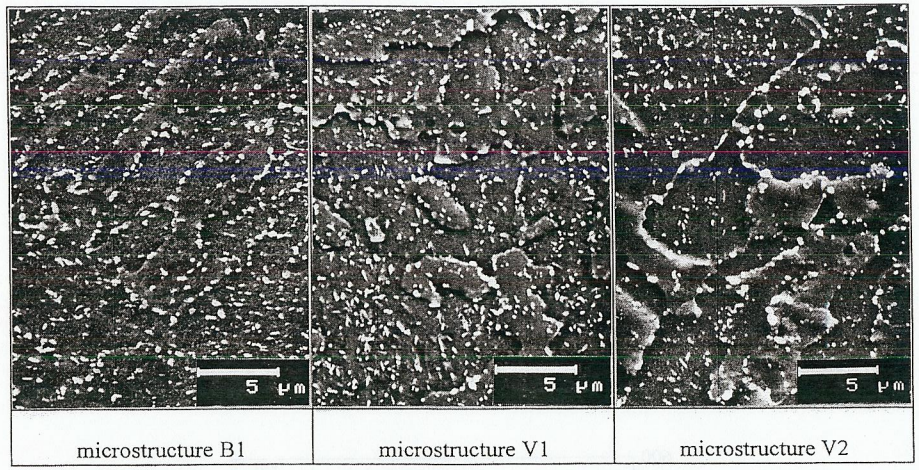

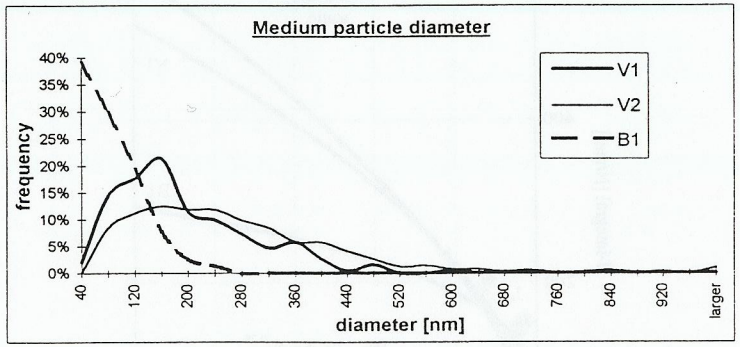

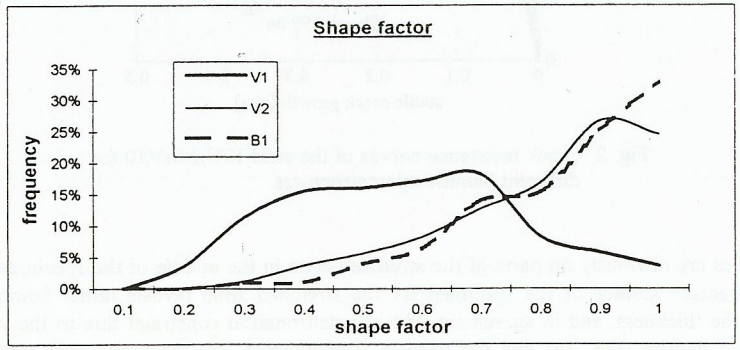

Fig. 1 Carbide distribution after different heat treatment

found rarely; the Mo-content of the analysed carbides was less than 2%. The thin foils were also used to study the dislocation arrangement and density.

For the estimation of the crack resistance curves by the multispecimen method precracked specimens were loaded by three point bending by a cross head rate of 0.5 mm/min. After different pre-loading the crack extension was marked by heat tinting (350°C, 1h) and after that the specimens were broken at appoximately -100°C. The measurement of the initial crack length a_o and the stable crack extension Δa was carried out in agreement with ESIS P2 -92 (1992) by means of 9 values over the specimen width. The critical stretched zone parameters SZW_c and SZH_c were measured by SEM using a computer pragramme.

RESULTS AND DISCUSSION

Fig. 2 shows the influence of the microstructure on the R-curves J-Δa. The obtained curves can be described by a power law fit $J = A \cdot \Delta a^{B}$, whereby the constants A and B demonstrate the slope of the curve for each microstructure.

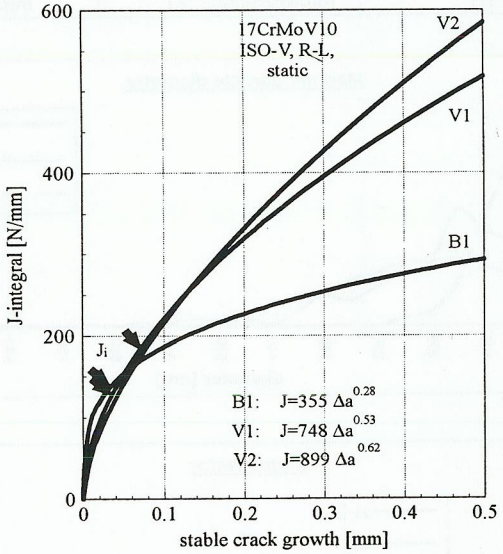

Fig. 2 Crack resistance curves of the steel 17CrMoV10 for different bainitic microstructures

Differences are obviously on parts of the stretched zone in the middle of the specimen (Fig.3) On the fracture surface of the specimen B1 the stretched zone reveals rather homogeneous through the thickness, and in agreement with the deformation constraint due to the very high dislocation density (Fig. 4a) and the particle strengthening by the very small carbides the smallest stretched zone with approximately the same SZW_c and SZH_c values was obtained.

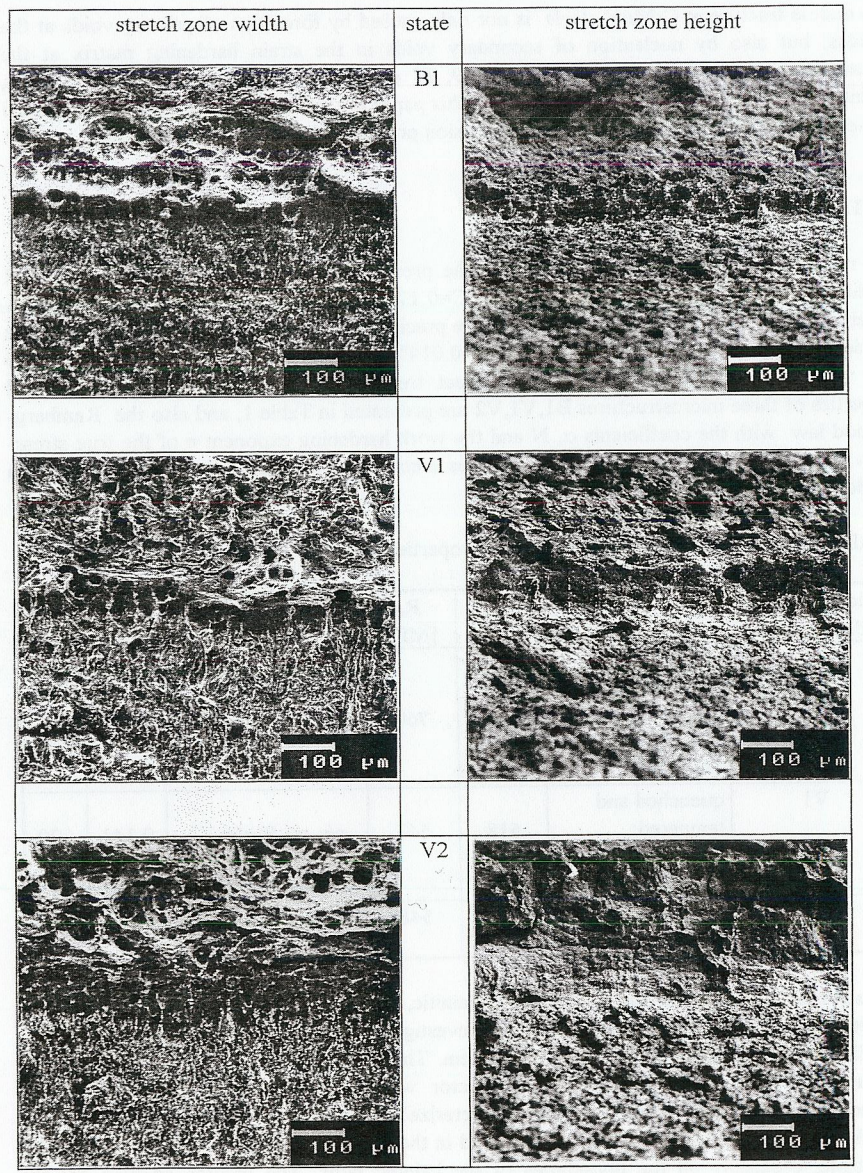

Fig. 3 SEM micrographs showing the critical stretch zone width and height at the mid-section thickness

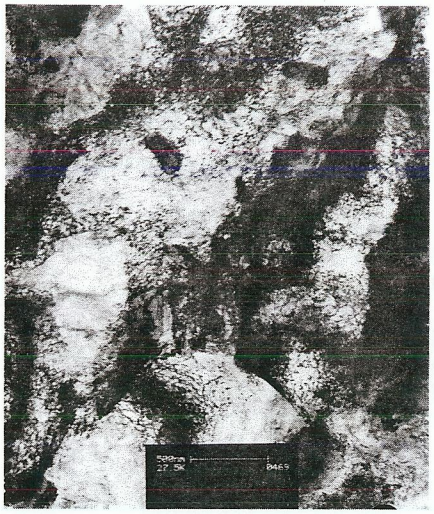

Fig. 4a Dislocation forest in the microstructure B1

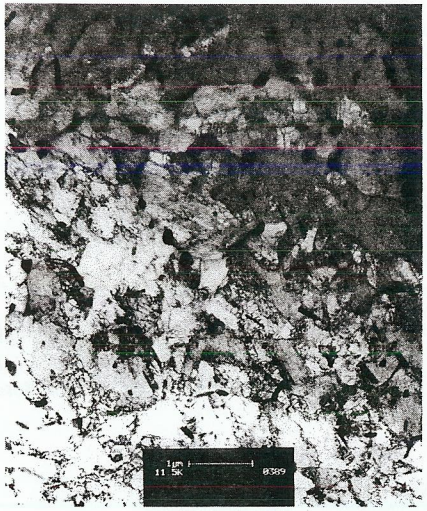

Fig. 4b Microstructure V1 with subgrains and low dislocation density

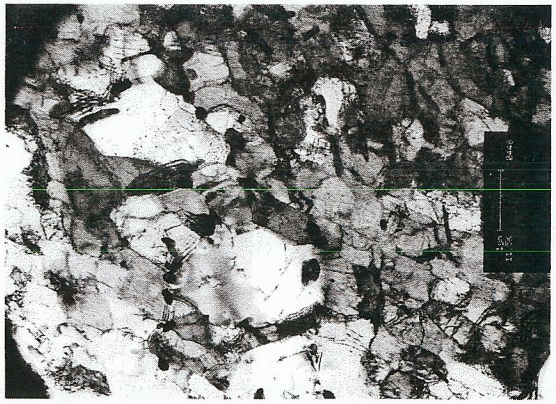

Fig. 4c Microstructure V2 with low energy configuration of dislocations

The critical stretched zone width and height and the ductile fracture parameters are presented in Table 2.

Table 2 Stretched zone and ductile fracture parameters

microstructure	SZW_c [µm]	SZH_c [µm]	J_i N/mm]	T_i	$T_{\Delta a=0.3}$
B_1	34	36	138	465	109
V_1	36	68	133	1172	548
V_2	75	70	180	1480	1365

Whereas in the conditions V1 and B1 the SZW_c values are nearly the same, SZH_c is considerably higher for V1. This result is consistent with the lower dislocation density and dislocation arrangement (Fig. 4b) predominantly in the boundaries of the grains and very small subgrains, partly also around the coarse carbides. The reduction in the work hardening capacity could be the reason for the higher deformation ability at the crack tip before crack initiation occurs.

The longtime annealing process to produce the microstructure V2 yielded to a well-defined substructure with dislocations rearranged into lower energy configurations by recovering (Fig. 4c). Therefore the development of the stretched zone is favoured by an intense slip band formation at the crack tip.

To characterize the crack extension resistance the tearing-modulus ($T=dJ/da\cdot E/R_F^2$) with $R_F = ½ (R_e + R_m)$ was taken into account. In Table 2 it is seen that the T-moduli at initiation T_i and in the crack extension region $T_{\Delta a = 0.3}$ are more influenced in comparison to the fracture initiation toughness J_i. After crack initiation in the microstructures V1 and V2 more energy dissipates by plastic deformation of the ligament between the voids around large inclusions. Substantially a step-like crack propagation and partly crack branching was observed.

CONCLUSIONS

The investigated treatments are suitable to achieve a range of microstructure with different features both in the ferritic matrix (grain and subgrain size, dislocation density and arrangement) and of the carbide precipitation (size and shape, volume fraction).

The stretched zone profile depends on the microstructure in agreement with the work hardening capacity; this led to essentially higher SZW_c and SZH_c values for the condition V2 in comparison to V1 and B1.

The tearing modulus shows a more distinct dependence on the microstructure as the crack initiation toughness J_i. Whilst the initiation toughness values for the microstructures V1 and B1

are nearly the same, differences between the T-values indicate the margin in the deformation ability of the different bainitic microstructure.

The crack initiation and the path of the growing crack in a bainitic microstructure is essentially determined by the carbides, especially by their influence on the free dislocation path and the work hardening capacity during the deformation process at the crack tip.

The authors greatly acknowledge the support by Deutsche Forschungsgemeinschaft Bonn.

REFERENCES

Deimel, P. and E. Sattler (1993). Relation between size and densitiy of nonmetallic inclusions and the J-integral at crack initiation. *Nucl. Engng. and Design.*, **144**, 9-21.

ESIS P2-92 (1992). ESIS procedure for determining the fracture behaviour of materials.

Holzmann, M., B. Vlach, J. Man and J. Krejci (1995). The influence of tempering on cleveage fracture and transition behaviour of bainitic 2.25Cr1Mo steel. *Steel research*, **66**, 264-271.

Li, G.C., T. Guennouni and D. François (1989). Influence of secondary void damage in the matrix material around voids. *Fatigue Fract. Engng. Mater. Struct.*,**12**, 105-122.

Parilák, L. and J. Dojcak (1993). Influence of microstructure on micromechanisms of failure in HSLA steels. *Int. J. Press. & Piping.*,**55**, 353-360.

Pointner, P. (1991). Umwandlungsverhalten und mechanische Eigenschaften des Stahles 41Cr4 im Bainitbereich. In: *Sonderband der Prakt. Metallographie*, **22**, 357-367, Riederer-Verlag Stuttgart.

Ridley, N., S. Maropoulas and J.D.H. Paul (1994). Effects of heat treatment on microstructure and mechanical properties of Cr-Mo-3,5Ni-V steel. *Mat. Sc. and Techn.*,**10**, 239-249

Sun, D.Z., W. Brocks and A. Hönig (1995). Simulation of the effect of secondary voids on ductile fracture process by using cell models. In: *Proc. ICM 7*, (A. Bakker, ed.), The Hague, 424-425.

Thomson, R.C. and H.K. Bhadeshia (1994). Changes in chemical compisition of carbides in 2,25Cr-1Mo power plant steel. Part 1 Bainitic microstructures. *Mat. Sc. and Techn.*, **10**, 193-204.

Tomita, Y. (1995). Effect of morphology of nonmetallic inclusions on fracture toughness of quenched and light-tempered 0.4C-Cr-Mo-Ni steels. *Z. Metallkd.*, **86**, 216-221.

Tveergard, V. (1989). On the analysis of ductile fracture mechanics. In: *Proc. ICF7*, (Salama, K. et al., ed.), Vol. 1, 159-179, Houston.